

Boston University

OpenBU

<http://open.bu.edu>

Boston University Theses & Dissertations

Boston University Theses & Dissertations

2023

Searching for novel LZTR1-interacting proteins

<https://hdl.handle.net/2144/48392>

"Downloaded from OpenBU. Boston University's institutional repository."

BOSTON UNIVERSITY

ARAM V. CHOBANIAN & EDWARD AVEDISIAN SCHOOL OF MEDICINE

Thesis

SEARCHING FOR NOVEL *LZTRI*-INTERACTING PROTEINS

by

RYAN RIPERT

B.S., University of Central Florida, 2021

Submitted in partial fulfillment of the

requirements for the degree of

Master of Science

2023

© 2023 by
Ryan Ripert
All rights reserved

Approved by

First Reader

Karen Symes, Ph.D.
Associate Professor of Biochemistry & Cell Biology

Second Reader

Benjamin Neel, MD, Ph.D.
Director Laura & Isaac Perlmutter Cancer Center
Professor of Medicine
NYU Grossman School of Medicine

ACKNOWLEDGMENTS

Working on this thesis was a great learning experience. I would like to thank Dr. Benjamin Neel for guiding me throughout this process and making this an interesting experience. I learned so much from him, and he was a great mentor this past year. I would also like to thank everyone in the Neel lab, especially the people who served as my mentors and provided me guidance along the way: Dr. Wei Wei, Dr. Mitchell Geer, Dr. Toshiyuki Araki, Dr. Kiyomi Araki, Connor Foster, Dr. Oscar Pundel, Dr. Abhishek Bhardwaj, Dr. Suman Mukhopadhyay, and Dr. Yi Ban. They created a welcoming environment and helped me through this process.

SEARCHING FOR NOVEL *LZTR1*-INTERACTING PROTEIN

RYAN RIPERT

ABSTRACT

Leucine Zipper-like Transcription Regulator 1 (*LZTR1*) is responsible for encoding a member of the BTB-Kelch superfamily, which interacts with the Cullin3 (CUL3)-based E3 ubiquitin ligase complex. Researchers have discovered mutations in *LZTR1* in glioblastoma, schwannomatosis, and Noonan syndrome. However, the exact function of *LZTR1* in cancer development or human growth remains unclear. A previous study in the Neel lab showed there was a cell-context dependent regulation of pan RAS (K/N/H RAS) levels by *LZTR1*. This thesis's main objective was to understand the underlying mechanisms for the above observation. The *LZTR1* gene has gained importance in human well-being due to its essential role in cellular activities and its link to various diseases. Investigating the range of functions of *LZTR1* and the underlying mechanisms will offer new perspectives on disease prevention and therapeutic approaches. These results provide hints for deciphering the mechanisms of RAS degradation and controlling the RAS/MAPK signaling pathway.

TABLE OF CONTENTS

ACKNOWLEDGMENTS	iv
ABSTRACT.....	v
TABLE OF CONTENTS.....	vi
LIST OF FIGURES	viii
LIST OF ABBREVIATIONS.....	ix
INTRODUCTION	1
Specific Aims.....	10
METHODS	11
PCR.....	11
Isolation of PCR products.....	12
Transformation of competent bacteria	14
Isolation of plasmid DNA from bacteria (Miniprep).....	14
Gibson assembly	15
Isolation of plasmid DNA from bacteria (Maxiprep)	16
Cell Culture.....	17
Packaging and concentration of lentiviruses	18
Lentiviral infection and selection of cell lines	18
TurboID expression and labeling	19
Isolation of biotinylated proteins	19
Western blotting.....	21

RESULTS	22
Cell line dependent upregulation of RAS family proteins upon <i>LZTR1</i> knockout.....	22
Generation of <i>LZTR1</i> -TurboID fusion construct	24
DISCUSSION.....	29
BIBLIOGRAPHY.....	35
CURRICULUM VITAE.....	42

LIST OF FIGURES

Figure 1. The proposed model for <i>LZTR1</i> function in the RAS/MAPK signaling pathway	3
Figure 2. <i>LZTR1</i> Mechanism of Action	3
Figure 3. Gibson Assembly.....	6
Figure 4. Plasmid Map of <i>LZTR1</i> tagged with TurboID.....	7
Figure 5. Biotin Ligase Labeling	9
Figure 6. Polymerase Chain Reaction.....	12
Figure 7. DNA Purification from Agarose Gels or Enzymatic Mix	17
Figure 8. <i>LZTR1</i> KO has cell context-dependent effects on RIT1 and RAS family members	23
Figure 9. The addition of biotin increases labeling in N-terminal TurboID-expressing cells	25
Figure 10. The addition of biotin had no significant effect on labeling in C-terminal TurboID-expressing cells.....	26
Figure 11. Model showing sites of action of <i>LZTR1</i>	30
Figure 12. A proposed schematic showing <i>LZTR1</i> functioning in a CRL3 complex that down-regulates RAS-MAPK signaling.....	32

LIST OF ABBREVIATIONS

BSA.....	Bovine Serum Albumin
BTB.....	Broad complex, Tramtrack, Bric a brac
BU.....	Boston University
Cas9.....	CRISPR-associated protein 9
cDNA.....	complementary DNA
CRLs.....	Cullin-RING ubiquitin ligases
CUL3.....	Cullin-3
DNA.....	Deoxyribonucleic acid
DNEM.....	Dulbecco's Modified Eagle's Medium
dNTP.....	Deoxynucleoside triphosphate
ERK.....	Extracellular signal-regulated kinase
GBM.....	Glioblastoma
GRB2.....	Growth Factor Receptor Bound Protein 2
GTP.....	Guanosine-5'-triphosphate
HEK.....	Human embryonic kidney
HRAS.....	Harvey rat sarcoma viral oncogene homolog
HRP.....	Horseradish peroxidase
INPPL1.....	Inositol polyphosphate phosphatase like 1
KBTBD7.....	Kelch repeat and BTB domain-containing protein 7
KEAP 1.....	Kelch-like ECH-associated protein 1
KOD.....	Thermococcus kodakaraensis

KRAS..... Ki-ras2 Kirsten rat sarcoma viral oncogene homolog
 LB Lysogeny Broth
LZTR1 Leucine Zipper-like Transcriptional Regulator 1
 MAP4K5..... Mitogen-Activated Protein Kinase Kinase Kinase Kinase 5
 MEK..... Mitogen-activated protein kinase kinase
 MEKK1..... Mitogen-activated protein kinase kinase kinase 1
 MRAS Muscle RAS oncogene homolog
 NF1 Neurofibromin 1
 NF- κ b Nuclear factor-Kappa B
 NRASNeuroblastoma RAS viral oncogene homologue
 NRF2.....Nuclear factor erythroid 2–related factor 2
 NS Noonan syndrome
 PBS Phosphate buffered saline
 PCR..... Polymerase Chain Reaction
 PD Pulldown
 PL..... Proximity labeling
 PMSF Phenylmethylsulfonyl fluoride
 PPP1CB..... Protein phosphatase 1 catalytic subunit beta
 PTPN11..... Protein tyrosine phosphatase non-receptor type 11
 PVDF Polyvinylidene difluoride
 RAF1.....Rapidly Accelerated Fibrosarcoma 1
 RAS/MAPK Rat sarcoma/mitogen-activated protein kinase

RIT1	RAS-like without CAAX 1
RPMI.....	Roswell Park Memorial Institute
RRAS	RAS-related protein
RTKs.....	Receptor tyrosine kinases
SDS-PAGE	Sodium dodecyl-sulfate polyacrylamide gel electrophoresis
SHP2	Src homology region 2-containing protein tyrosine phosphatase 2
SOS1	Son of Sevenless 1
TBS	Tris-buffered saline
TBST.....	Tris-buffered saline with 0.1% Tween® 20 detergent
UPS	Ubiquitin–proteasome system
WCL.....	Whole cell lysate

INTRODUCTION

The RAS/MAPK (Rat sarcoma/Mitogen-Activated Protein Kinase) pathway regulates cellular processes, such as cell proliferation and survival (Yuan et al., 2020). It is vital in transmitting signals from the cell membrane to the nucleus in response to extracellular stimuli, such as growth factors and hormones (Guo et al., 2020). Dysregulation of the RAS/MAPK pathway is frequently observed in various cancers, often due to mutations in crucial pathway components.

A critical RAS/MAPK pathway component is a non-receptor protein tyrosine phosphatase called SHP2. The protein tyrosine phosphatase non-receptor type 11 (PTPN11) gene encodes for SHP2. The SHP2 protein is a critical positive RAS/MAPK pathway regulator. SHP2 can bind to various receptor tyrosine kinases (RTKs) and other signaling molecules, which allows it to regulate the RAS/MAPK pathway (Neel et al., 2003).

Recently during Wei et al. (2023) CRISPR screen, a novel gene called Leucine Zipper-like Transcriptional Regulator 1 (*LZTR1*) was identified as a significant contributor to resistance to SHP2 inhibitors. *LZTR1* is a tumor suppressor gene first discovered as a gene that undergoes deletion in most DiGeorge syndrome patients (Piotrowski et al., 2014). *LZTR1* is associated with the Golgi matrix and could potentially regulate the function of the Golgi apparatus (Zhang et al., 2021a). The Golgi apparatus is responsible for the processing, sorting, and delivering proteins and plays a vital role in cancer (Zhang et al., 2021a).

Furthermore, *LZTR1* has been shown to interact with Cullin-RING ubiquitin ligases (CRLs) (Abe et al., 2020; Bigenzahn et al., 2018; Steklov et al., 2018). CRLs are multi-protein complexes that function as ubiquitin ligases (Paladino et al., 2021). *LZTR1* functions as an adaptor protein in the Cullin-RING ligase 3 (CRL3) complex, which is a part of the ubiquitin-proteasome system (UPS) responsible for protein degradation (Paladino et al., 2021; Zhang et al., 2021a). *LZTR1* facilitates the recruitment of specific substrates to the CRL3 complex, such as the RAS family of proteins (Motta et al., 2019).

Moreover, *LZTR1* regulates the RAS-MAPK signaling pathway (Zhang et al., 2021b). Previous studies have reported that *LZTR1* is responsible for the polyubiquitination and degradation of RAS through the ubiquitin-proteasome pathway, inhibiting RAS/MAPK signaling (Abe et al., 2020; Castel et al., 2019). Additionally, *LZTR1* hinders the RAS/MAPK signaling pathway, whereas *LZTR1* loss of function mutations lose this capability, leading to the overactivation of RAS/MAPK signaling (Zhang et al., 2021a). Mutations in *LZTR1* have been linked to an increased risk of cancer. Overall, pathological *LZTR1* mutations are defective in facilitating substrate ubiquitination by interrupting the formation of substrate-*LZTR1*-CUL3 complexes (Zhang et al., 2021a).

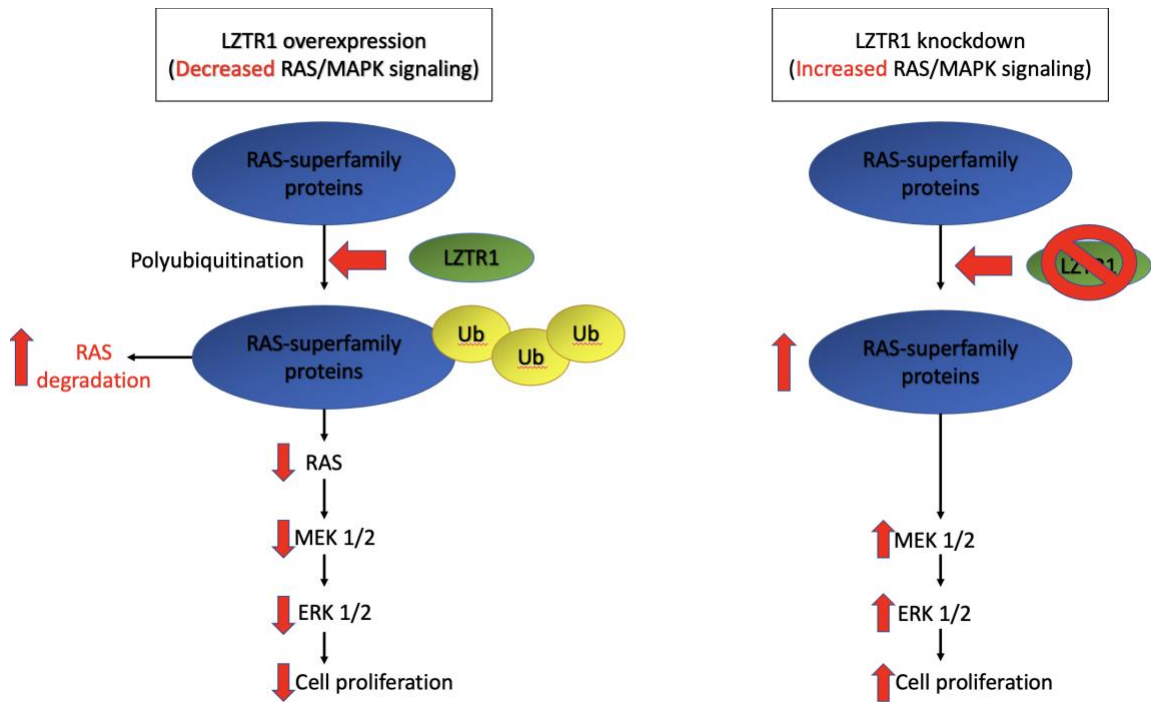


Figure 1. The proposed model for *LZTR1* function in the RAS/MAPK signaling pathway. RAS/MAPK signaling regulates cell proliferation. (Adapted from Abe et al., 2020)

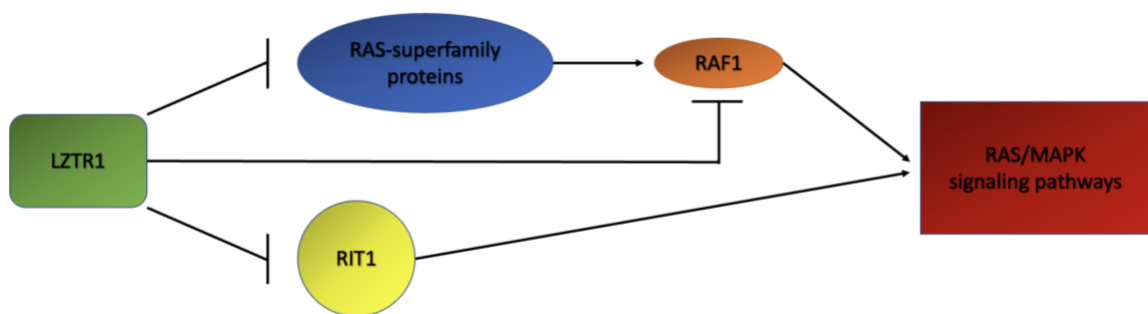


Figure 2. *LZTR1* Mechanism of Action. *LZTR1* indirectly regulates RAS/MAPK signaling, and mutations in *LZTR1* or RAS-superfamily proteins lead to the overactivation of the RAS/MAPK signaling pathway. (Adapted from Zhang et al., 2021)

LZTR1 is a multifunctional protein with significant roles in several biological processes. Its involvement in human disease makes it a crucial target for therapeutic intervention. Further research into its functions could lead to a better understanding of cellular regulation and disease pathology. Recently, mutational analyses elucidated the role of pathological *LZTR1* mutations in the RAS/MAPK signaling pathway, and *LZTR1* has been discovered by mass spectroscopy to interact with a RAS-related small GTPase, RIT1, an oncoprotein extensively involved in Noonan syndrome (NS) and cancer (Castel et al., 2019; Paladino et al., 2021). Castel et al. (2019) demonstrated that, under physiological conditions, *LZTR1* stimulates RIT1 proteolysis through CUL3-mediated proteasomal degradation, while pathogenic mutations affecting RIT1 or *LZTR1* lead to RIT1 upregulation and promote the overactivation of MAPK signaling. Therefore, a better comprehension of the mechanism would aid in elucidating the role of *LZTR1* in pathological diseases, consequently encouraging advancement in developing innovative therapeutic approaches (Paladino et al., 2021).

Genetic analysis has determined that almost all NS-associated RIT1 mutants lose their ability to interact with LZTR1 compared with the wild-type RIT1, leading to the reduction of the degradation of RIT1 mutants (Zhang et al., 2021a). Under physiological conditions, RIT1 is ubiquitinated by the LZTR-CUL3 complex, then degraded by the UPS (Zhang et al., 2021a). The UPS is a critical component for maintaining cellular homeostasis, and its dysregulation has been implicated in various human diseases (Park et al., 2020). Moreover, under pathological conditions, RIT1 avoids UPS-mediated degradation, thus significantly enhancing MAPK signaling in NS (Zhang et al., 2021a).

The involvement of *LZTR1* in the ubiquitination and the progression of various diseases make this protein an appealing therapeutic target (Castel et al., 2019).

Ubiquitination is a vital post-translational modification that significantly impacts the homeostasis of the intracellular environment, cell growth, differentiation, and other cellular functions. A disproportion in protein degradation mediated by ubiquitination can be the molecular basis for specific human diseases, such as cancers. Indeed, *LZTR1* germline and somatic mutations have been found in patients with schwannomatosis and glioblastoma.

Furthermore, *LZTR1* mutations have been associated with Noonan syndrome. Noonan syndrome is a relatively prevalent autosomal dominant or recessive inherited disorder depicted by congenital heart defects, intellectual disability, and elevated cancer risk. Noonan syndrome and related conditions are known as RASopathies, caused by germline mutations in genes encoding various RAS/MAPK signaling pathway components. Considering the direct structure-activity relationships, a deeper understanding of its molecular structure and determining molecular parameters characteristic of protein-protein interactions are crucial (Castel et al., 2019). This information can differentiate between various molecular states, identify the active conformation of the tumor suppressor capable of recruiting substrates, and predict other possible interactors.

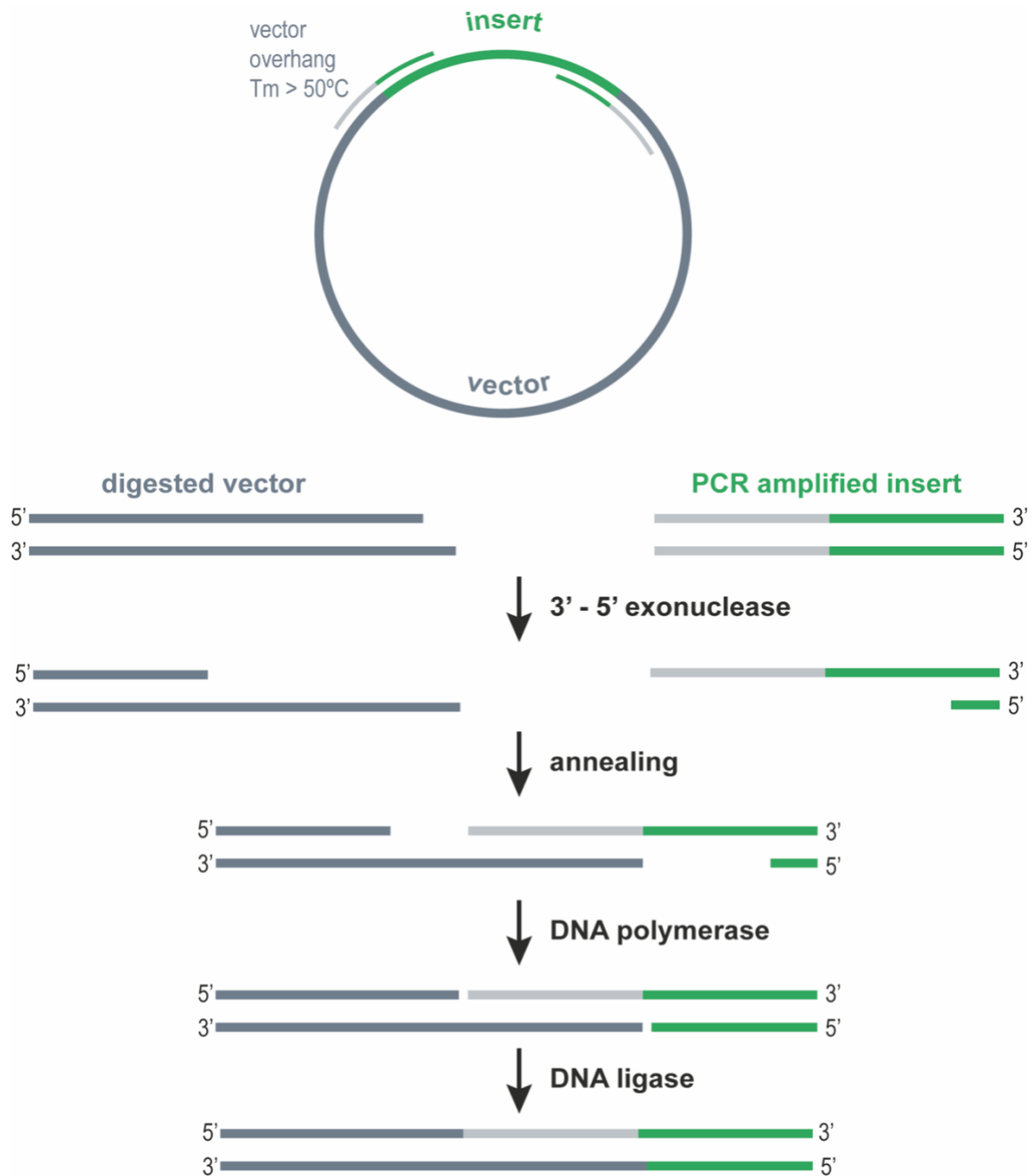


Figure 3. Gibson Assembly. Gibson Assembly combines one or more inserts with a vector more efficiently than DNA ligation. (Attained from Mitchell Geer)

In this study, the *LZTR1* gene and "TurboID" were cloned into a plasmid using Gibson Assembly, a method for molecular cloning established explicitly to join several

DNA fragments. This method is based on assembling overlapping DNA fragments and then joining them using three enzymes: a 5' exonuclease, a DNA polymerase, and a DNA ligase, in an isothermal reaction. It is a highly efficient, accurate, and rapid cloning and genetic engineering method. The Gibson Assembly protocol streamlines the cloning process by simultaneously assembling multiple DNA fragments in a single reaction without the need for restriction enzymes or ligases, making it a popular choice for molecular biology and synthetic biology applications.

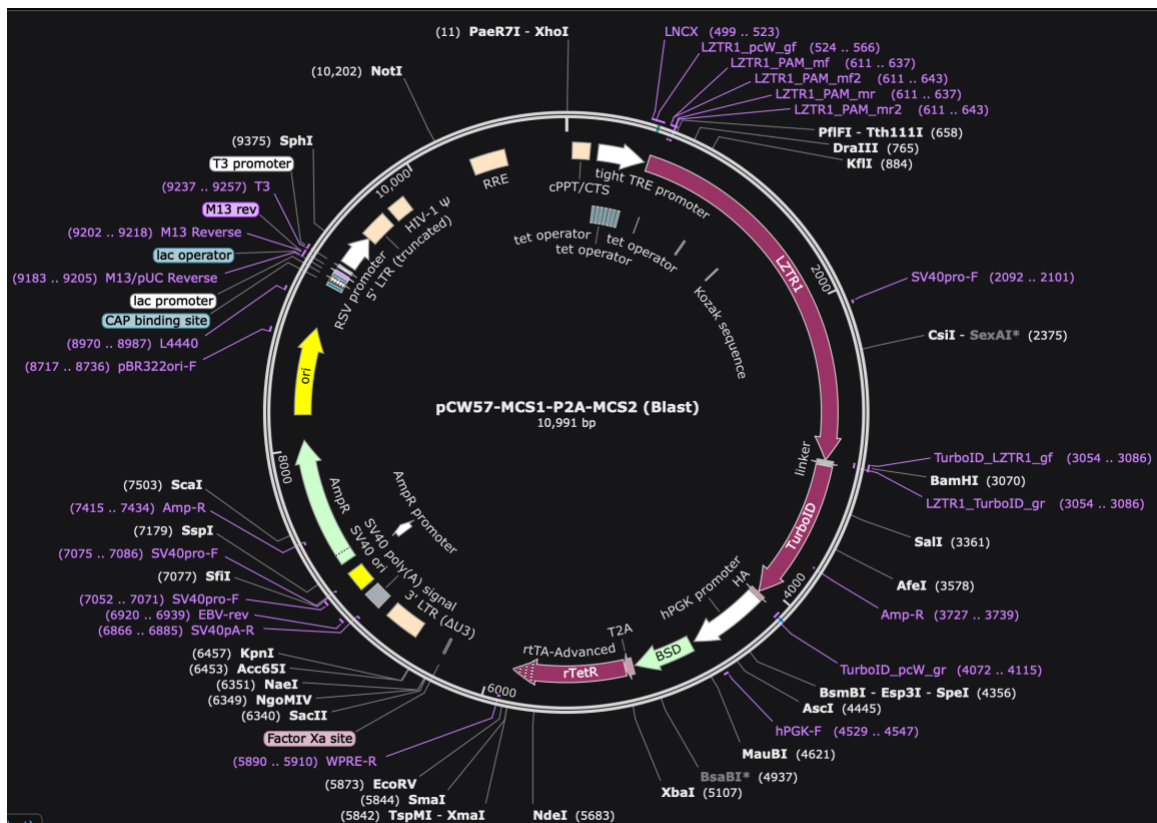


Figure 4. Plasmid Map of LZTR1 tagged with TurboID. The vector was pCW57-MCS1-P2A-MCS2 with Blasticidin resistance. The LZTR1 insert is approximately 2.5 kb, and the TurboID insert is ~1 kb

The plasmid created from the Gibson Assembly is being used to investigate the protein interactions of *LZTRI* using proximity labeling (PL), which enables the proteins that interact with *LZTRI* in living cells to be observed. PL has been useful in many cell types to analyze the protein components (Cho, Branon, Udeshi, et al., 2020). In PL, a promiscuous labeling enzyme is directed by genetic fusion to a specific protein (Branon et al., 2018). The addition of biotin initiates the covalent tagging of endogenous proteins within a few nanometers of the promiscuous enzyme (Branon et al., 2018). Then, the biotinylated proteins are isolated using streptavidin-coated beads and characterized by mass spectrometry (Cho, Branon, Rajeev, et al., 2020). Biotin molecules tightly bind to streptavidin proteins. The high affinity and specificity of biotin for streptavidin have been used to isolate multiple molecules. These labeled molecules can then be identified and analyzed, providing insights into their interactions and localization within the cell (Shioya et al., 2022). Biotin labeling technology is an essential tool in molecular biology.

Earlier PL methods (e.g., BioID) required extensive labeling time or utilized chemicals with low cell permeability or high toxicity (Branon et al., 2018). TurboID is a promiscuous mutant of biotin ligase that catalyzes PL with much greater efficiency than BioID and enables 10-min PL in cells with non-toxic and easily deliverable biotin (Branon et al., 2018).

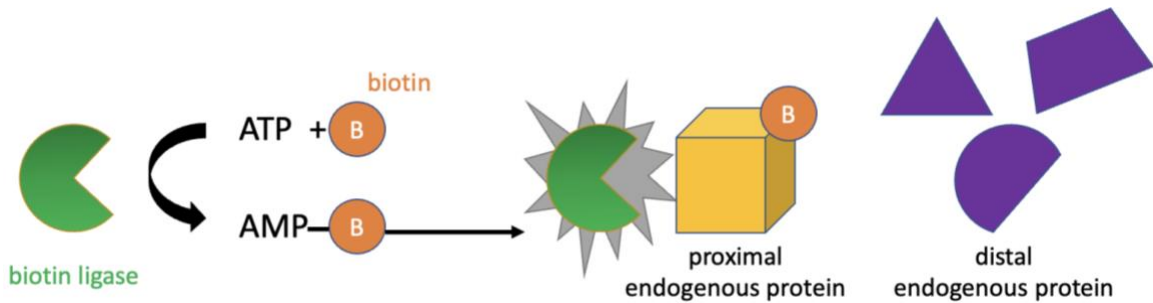


Figure 5. Biotin Ligase Labeling. Biotin ligase labels only proximal endogenous proteins with biotin. (Adapted from Branon et al., 2017)

TurboID is an engineered enzyme derived from the biotin ligase BirA found in *Escherichia coli*. It has been optimized for rapid and efficient labeling of proximal proteins. TurboID has enhanced catalytic activity, allowing it to biotinylate proteins within its vicinity much more rapidly than the wild-type BirA enzyme. This enables researchers to conduct proximity labeling experiments within shorter time frames (e.g., minutes to hours) than traditional methods, which might require 18–24 hours or more.

The TurboID approach is advantageous for studying weak or transient protein-protein interactions, which may be difficult to detect using traditional co-immunoprecipitation or pulldown assays (Qin et al., 2021; X. Wei et al., 2023). By fusing the TurboID enzyme to a protein of interest, researchers can biotinylate nearby proteins within living cells, facilitating the identification of interaction partners and revealing potential functions and cellular localization of the protein of interest.

As previously mentioned, the findings from the Neel lab have shown that loss of *LZTR1* expression, using CRISPR-Cas9 mediated knockout, led to resistance against SHP2 inhibitors in multiple cell lines (W. Wei et al., 2023). In line with observations from Castel et al. (2019), RIT1 levels increased in all tested *LZTR1* knockout (KO) cell

lines. Similarly, increased muscle RAS oncogene homolog (MRAS) levels were observed in almost all *LZTR1*-deficient lines. However, increased levels of other RAS proteins were cell line-dependent. For instance, in MV4-11 cells, the levels of KRAS, NRAS, and HRAS remained unaltered by *LZTR1* KO. By contrast, in K562 cells, *LZTR1* deficiency led to increased KRAS, HRAS, NRAS, and RAS-related (RRAS) levels, alongside the typical elevation of RIT1 and MRAS. These results suggest that specific RAS family members act as conditional substrates depending on the cell context (W. Wei et al., 2023). The most straightforward explanation for these findings is that *LZTR1/CUL3* complexes contain additional components to be identified. The primary goal of this thesis is to identify novel *LZTR1* interactors using the TurboID approach.

Specific Aims

I hypothesize that different *LZTR1/CUL3* complexes are present in MV-411 and K562 cell lines, leading to the differential regulation of RIT1/MRAS and KRAS/HRAS/NRAS/RRAS. The different complexes likely fall into one of the following categories:

1. A protein is expressed in K562 cells, which is absent in MV-411 cells, that recruits KRAS/HRAS/NRAS/RRAS to the *LZTR1/CUL3* ubiquitin ligase complex
2. A protein is expressed in MV-411 cells, which is absent in K562 cells, that prevents KRAS/HRAS/NRAS/RRAS recruitment to the *LZTR1/CUL3* ubiquitin ligase complex

METHODS

PCR

Forward and reverse primers were designed, using the Agilent QuikChange Primer design tool, to insert silent mutations into the Cas9 PAM recognition site. A sample reaction mixture was prepared following the instructions of the KOD Xtreme Hot Start DNA Polymerase kit. The PCR reaction mix, which included template DNA, forward and reverse primers, dNTPs, deionized water, 2X Xtreme Buffer, and KOD Xtreme Hot Start DNA Polymerase, were combined in a PCR tube. The mixture was vortexed and briefly centrifuged to ensure it settled at the bottom of the tube before being placed in a thermal cycler.

The PCR reaction proceeded through several stages. First, the KOD Xtreme Hot Start DNA Polymerase was activated by heating it to 94°C for two minutes. Next, denaturation occurred at 98°C for ten seconds. The temperature was then lowered to the Lowest Primer T_m°C for thirty seconds, allowing the primers to anneal to the template DNA. Finally, the extension stage took place at 68°C for 1 minute per kilobase pair, where the KOD Xtreme Hot Start DNA Polymerase incorporated free dNTPs into the template DNA to create the PCR product. This process was repeated for 30 cycles, consisting of denaturation, annealing, and extension phases. Upon completion of the PCR reactions, the mixtures were cooled to 4°C.

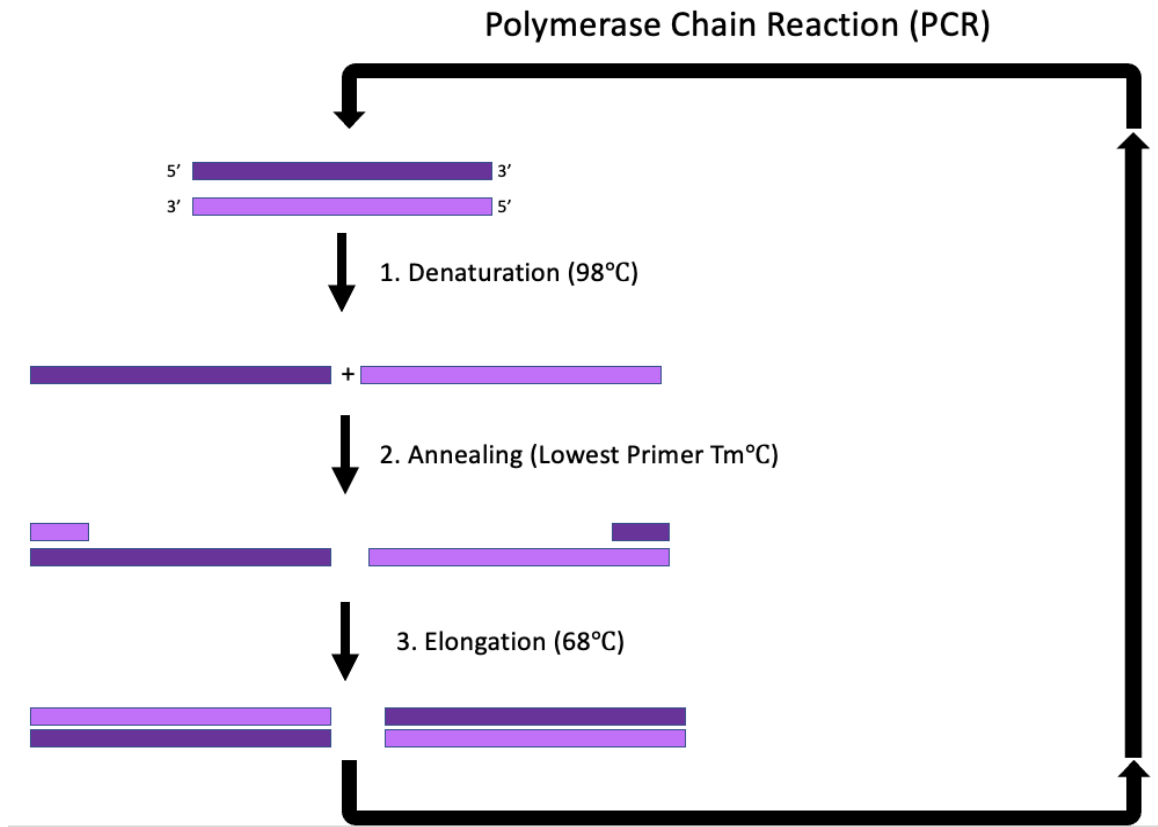


Figure 6. Polymerase Chain Reaction. The DNA stranded undergoes denaturation, annealing, then elongation for 25–40 cycles. (Adapted from Garibyan & Avashia, 2013)

Isolation of PCR products

The GFX PCR DNA and Gel Band Purification kit isolated and purified the target PCR product from the PCR reaction. A 500 μ L volume of Capture Buffer Type 3 was thoroughly combined with the 50 μ L PCR product in a microcentrifuge tube. After centrifuging the mixture to gather the liquid at the tube's bottom, it was loaded onto the assembled GFX MicroSpin column and Collection tube. The assembly was then

centrifuged at $16,000 \times g$ for 30 seconds, and the flow-through was discarded by emptying the collection tube. The GFX MicroSpin column was reinserted into the collection tube.

Next, $500\mu\text{L}$ of Wash Buffer Type 1 was added to the GFX MicroSpin column, and the assembly was centrifuged at $16,000 \times g$ for 30 seconds. The collection tube was discarded, and the GFX MicroSpin column was placed in a new, DNA-free 1.5 ml Eppendorf tube. Subsequently, $20\mu\text{L}$ of Elution Buffer Type 4 was added to the assembled GFX MicroSpin column and sample collection tube, followed by incubation at room temperature for 1 minute. Lastly, the assembly was centrifuged at $16,000 \times g$ for 1 minute to retrieve the plasmid.

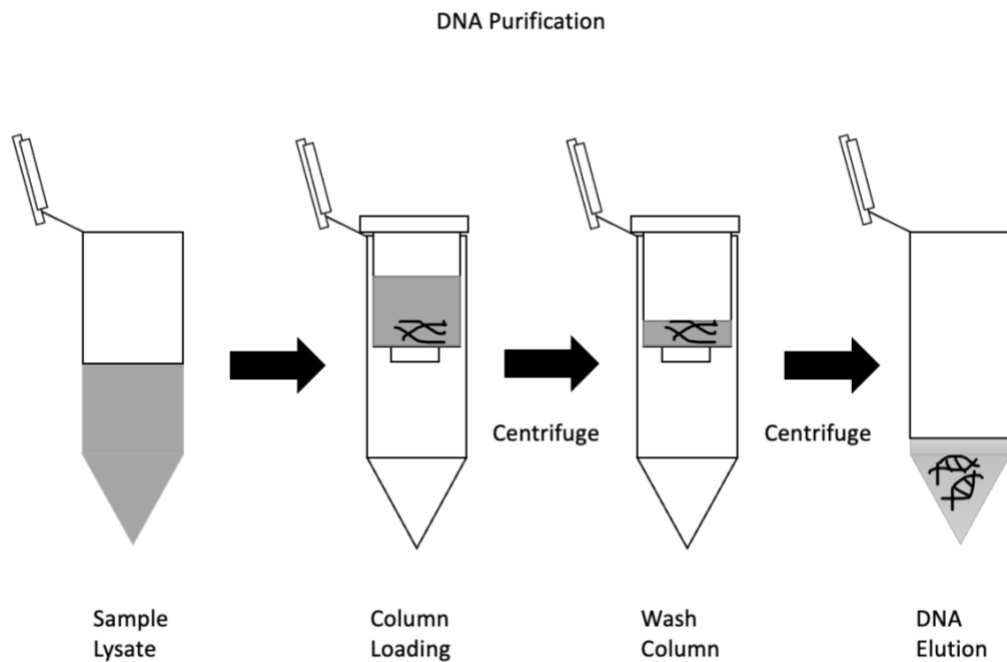


Figure 7. DNA Purification from Agarose Gels or Enzymatic Mix. A schematic showing the steps to DNA isolation from a lysate (Adapted from Barbosa et al., 2016)

Transformation of competent bacteria

After PCR DNA purification, the plasmid was used to transform competent cells for propagation and DNA extraction. A 10ng/ μ L plasmid concentration was added to the competent cells, which were then mixed and incubated on ice for 30 minutes. The cells were subjected to heat shock at 42°C for 45 seconds to help with plasmid DNA uptake. Following heat shock, the cells were placed back on the ice for a short recovery period. The transformed cells were allowed to recover and express the spectinomycin antibiotic resistance gene found on the plasmid. They were incubated in LB broth at 37°C for one hour to repair membranes and initiate resistance gene expression. The cells were then plated on a spectinomycin-selective agar plate and incubated overnight at 37°C to produce individual colonies.

Isolation of plasmid DNA from bacteria (Miniprep)

Several colonies were picked and grown overnight in 2mL LB broth with spectinomycin. Following the instructions of the Wizard® Plus SV Minipreps DNA Purification System kit, a bacterial lysate was prepared. Next, the bacterial lysate was centrifuged at maximum speed in a microcentrifuge for 10 minutes at room temperature. The lysate was transferred to a spin column inside a 2mL collection tube and centrifuged at maximum speed for 1 minute. The flow-through was discarded, and the spin column was returned to the collection tube. Then, 750 μ l of wash buffer, diluted with 95% ethanol, was added to the spin column, followed by another round of centrifugation. The washing process was repeated with 250 μ l of wash buffer. The collection tube was then

centrifuged for 2 minutes at maximum speed.

The spin column was transferred to a sterile 1.5ml Eppendorf tube, and 100µl of Nuclease-Free Water was added to elute the plasmid DNA. The collection tube was centrifuged at maximum speed for 1 minute, and the spin column was removed. DNA purity and concentration were assessed using a NanoDrop, and the results were recorded. Finally, the plasmid DNA was sent for Sanger sequencing to confirm successful PAM site mutagenesis.

Upon confirmation of the introduction of the mutation of interest, we used the mutant plasmid as the template DNA for all further *LZTR1* PCRs. Another plasmid was used to obtain the TurboID insert DNA. PCR was conducted to amplify the genes of interest. The PCR products mixed with loading dye were loaded into the wells of a 1% agarose gel containing ethidium bromide, and gel electrophoresis was performed at 120V for 30 minutes. Then the gel was visualized under low-intensity UV light, and the desired DNA fragments were excised using a scalpel. PCR products were isolated and purified using the GFX PCR DNA and Gel Band Purification kit.

Gibson assembly

The *LZTR1* and TurboID DNA fragments were employed in Gibson assembly to create the final expression plasmid. This reaction used the two DNA fragments, an in-house Gibson Assembly Master Mix (including 5' exonuclease, Taq polymerase, DNA ligase, and dNTPs), and deionized water ("Isothermal Reaction (Gibson Assembly) Master Mix," 2017). After combining the DNA fragments, Gibson Assembly Master

Mix, and deionized water in a PCR tube, the tube was placed in a thermocycler at 50°C for 30 minutes. Then transformed competent *E. coli* with the reaction product, plated them on LB agar plates with ampicillin, and incubated them overnight. Positive colonies were inoculated into a liquid culture and grown overnight, and the plasmid DNA was isolated from the bacterial culture using the Wizard® Plus SV Minipreps DNA Purification System.

The colonies were screened using sequencing primers and primers designed to bind to the two insert DNAs. DNA samples were sent for Sanger sequencing to ensure the collected DNA contained the inserts.

Isolation of plasmid DNA from bacteria (Maxiprep)

Once the plasmid was verified by Sanger sequencing, a Maxiprep was conducted to obtain enough plasmid DNA for transduction. The plasmid from the Miniprep was used to transform competent cells, which were then inoculated into 200 mL of LB broth with ampicillin and incubated overnight at 37°C with shaking at 250 rpm. The bacterial culture was centrifuged at 6,000 g for 15 minutes at 4°C to pellet the cells. The supernatant was decanted, and the bacterial pellet was resuspended in 10 mL of Buffer P1. Then, 10 mL of Buffer P2 was added and mixed by inverting the tube four times. The tube was incubated at room temperature for 5 minutes.

After that, 10 mL of cold Buffer P3 was added and mixed by inverting the tube four times. The tube was placed on ice for 15 minutes and then centrifuged at 20,000 g for 30 minutes at 4°C to pellet the precipitate. The supernatant was carefully decanted

into a sterile tube. The QIAGEN-tip 500 was equilibrated by applying 10 mL of Buffer QBT, allowing it to pass through the tip by gravity flow. The lysate was added to the QIAGEN-tip 500, allowing it to enter the resin by gravity flow. The QIAGEN-tip 500 was washed by applying 30 mL of Buffer QC, allowing it to pass through the tip by gravity flow. The plasmid DNA was eluted from the QIAGEN-tip 500 using 15 mL of Buffer QF and collected into a clean container.

Next, 10.5 mL of room-temperature isopropanol was added to the eluted DNA, mixed gently, and incubated at room temperature for 5 minutes. The supernatant was carefully decanted, and the DNA pellet was washed with 5 mL of room temperature 70% ethanol. The sample was centrifuged at 15,000 g for 10 minutes at 4°C, the supernatant was carefully decanted, and the pellet was air-dried for 10–20 minutes. Finally, the dried plasmid DNA pellet was dissolved in 1 mL of nuclease-free water.

Cell Culture

Cells were maintained in 5% CO₂ at 37°C in media conditions described by the vendor or the source laboratory and were tested monthly for mycoplasma by PCR (Young et al., 2010). KO cells were generated by infection with lentiviruses constitutively expressing Cas9 and appropriate sgRNAs. All experiments were performed with early passage lines within 3 min of defrosting. MV4-11 and K562 cells were attained from Dr. Wei Wei (NYU Grossman School of Medicine, New York, NY, USA) in June 2020. MV4-11 and K562 were cultured in RPMI supplemented with 10% FBS and 1% penicillin/streptomycin.

Packaging and concentration of lentiviruses

Three million HEK 293 cells were plated onto a 10 cm cell culture dish for transduction. The media of the HEK cell was changed to DMEM+10% FBS. In a sterile Eppendorf tube, 500 μ L pre-warmed OptiMEM was mixed with three plasmids: 5 μ g of the turbo-*LZTR1* plasmid, 3 μ g psPAX2, and 2 μ g pMD2.G. The plasmids were mixed by inverting the tubes several times, and 30 μ L X-tremeGENE reagent was added and inverted several times. Then, the mix was incubated at room temperature for 20 minutes and added drop-wise with a 1mL pipette to the HEK cells. The media of the HEK cell was changed with 1 ml fresh DMEM+10% FBS+1% P/S, and 1 ml FBS was added. The cells were placed in the incubator for two days.

After 48h incubation, the supernatant was removed and filtered with a 45 μ m pore size filter to eliminate the cell debris. The filtered supernatant was mixed with a 3.5 mL Lenti-X concentrator and stored at 4°C overnight. The mixture was centrifuged at 1500g for 45 mins at 4°C to precipitate the virus. The supernatant was removed, and the virus pellet was resuspended in 1 mL of RPMI, aliquoted into tubes, and frozen at -80°C.

Lentiviral infection and selection of cell lines

MV4-11 and K562 cells were cultured to have 10 million cells. In a 6-well plate, 7 million cells were placed in 2 ml media in one well, and 450 μ L of the virus were added to MV4-11 and 50 μ L to K562. Two (2) μ L of 4mg/ml polybrene were added into each well. The plate was then centrifuged at room temperature at 1500g for one hour and transferred to the incubator overnight. The next day, the cells were removed and

resuspended in 10 ml of media in a 10 cm dish. After two days, blasticidin was added to select transduced cells. For MV4-11, 30 $\mu\text{g/ml}$ of blasticidin were added. For K562, 500 $\mu\text{g/ml}$ of blasticidin were added. The media was refreshed with antibiotics every two days until day 8. Then the cells were expanded, and aliquots of cells were frozen for future use.

TurboID expression and labeling

Expression of TurboID fusion proteins were induced by exposing cells to doxycycline in biotin-free media for three days. Then, 500 μM biotin was added to the culture medium to label cells for 15 mins at 37°C. The labeling was stopped by washing cells in ice-cold PBS at least three times. The cells were pelleted into 1.5 ml Eppendorf tubes, the PBS was removed, and the cells were lysed immediately on ice in RIPA buffer with protease and phosphatase inhibitors for 15 minutes. The lysate was then centrifuged at 10,000 g for 10 minutes at 4°C to pellet cell debris, and 100 μL of supernatant were removed and boiled in 5x reducing sample buffer, labeled as the WCL sample.

Isolation of biotinylated proteins

A magnet was placed on ice, and 100 μL of streptavidin beads were added to each tube for the pulldown (PD) samples. Tubes containing the beads were placed onto the cold magnet and allowed to separate for 3 minutes. The liquid was aspirated, and the beads were washed twice with 1 ml of RIPA buffer without inhibitors. Fully resuspended beads were then placed back on the magnet.

The calculated volume of lysate was added to the washed beads on ice, and RIPA buffer with inhibitors was added to normalize the volume of the lysates with beads. The samples were placed in a cold room to mix end-over-end for three hours. The samples were placed on the magnet for 3 minutes to separate the beads. One hundred (100) μL of lysate were removed and boiled in a reducing sample buffer, labeled as the post-pulldown sample. The remaining supernatant was aspirated, and the beads were washed three times with 1 ml of RIPA lysis buffer, resuspended in the lysis buffer, and placed back on the magnet. The s buffer was aspirated, 30 μL of 2x reducing sample buffer were added, and the samples were boiled. The WCL and PD samples were electrophoresed on the same gel to assess the enrichment of the samples and to ensure that the beads were in sufficient excess to capture all biotinylated proteins.

For Western blots, MV4-11 and K562 cells were placed into six-well plates at a concentration of 1 million cells/ml for a total volume of 2 ml. Cells were incubated overnight at 37C. The cells were removed from the incubator, placed on ice, and transferred into 5ml Eppendorf tubes and pellet at 1200 rpm for three minutes at 4°C. The tubes were placed on ice, and the supernatants were removed by vacuum aspiration. Pellets were resuspended in 1.5 ml Eppendorf tubes in 1mL cold PBS and placed on ice, and then centrifuged again at 1200 rpm for 3 minutes at 4°C. The tubes were placed on ice. The PBS was removed with an aspirator, and the cells lysed in modified RIPA buffer (50 mM Tris-HCl pH 8, 150 mM NaCl, 2 mM EDTA, 1% NP-40, and 0.1% SDS) containing 1mM of sodium beta-glycerophosphate, 2.5mM of sodium pyrophosphate, 100 μL Antipain, 100 μL PMSF, 100 μL Na₃VO₄, 100 μL NaF, 10 μL Aprotinin, 10 μL

Leupeptin, 10 μ L pepstatin. An appropriate amount of lysis buffer was used to lyse the cells. Lysates were incubated on ice for 15mins, centrifuged at 4°C for 30 mins, transferred into a new, labeled 1.5 ml Eppendorf tube, and put on ice.

Protein concentrations were determined by Coomassie blue assay. 5X sample buffer was then added to each sample and mixed. Proteins were resolved by SDS-PAGE and transferred to nylon membranes for 2 hr at 80V at 4°C

Western blotting

After the transfer, membranes were washed in ultrapure water and incubated for 1hr at a room temperature of 5% BSA in TBST. A primary antibody was added, and blots were incubated with shaking overnight in the cold room. The membranes were then quickly washed twice for 1 min and slowly washed three times for 5 min. Then, secondary antibodies were added (goat anti-mouse or goat anti-rabbit, as appropriate) both at 1:10,000 dilution in secondary antibody buffer (0.05% triton, 0.01% SDS, in TBS). Membranes were incubated at room temperature for one hour with shaking, then were quickly washed three times, followed by a slow wash three times. The membranes were allowed to dry in the dark and then imaged by ECF using a LICOR.

RESULTS

Cell line dependent upregulation of RAS family proteins upon *LZTR1* knockout

Through a CRISPR screen, Wei *et al.* (2023) showed that *LZTR1* knockout results in SHP2 inhibitor resistance in multiple cancer cell lines of various tissue types. Deletion of *LZTR1* with individual sgRNAs led to resistance against SHP2 inhibitors. Previous studies reported that *LZTR1* enhances the turnover of RAS family members or RIT1 by recruiting a CUL3 ubiquitin ligase complex. Germline mutations in *LZTR1* have been linked to some cases of Noonan syndrome. In light of the uncertainty surrounding the target of the *LZTR1*-containing ubiquitin ligase complex, RIT1 and RAS family member levels were examined in K562 and MV4-11 cells. In agreement with Castel *et al.* (2019), RIT1 levels increased in both tested *LZTR1* KO lines. Elevated MRAS levels were also observed in both K562 and MV4-11 cells.

In contrast, increased levels of other RAS proteins were cell-specific. For instance, in MV4-11 cells, the KRAS, NRAS, and HRAS levels remained unchanged by *LZTR1* KO. However, in K562 cells, *LZTR1* deficiency led to increased KRAS, HRAS, NRAS, and RRAS levels.

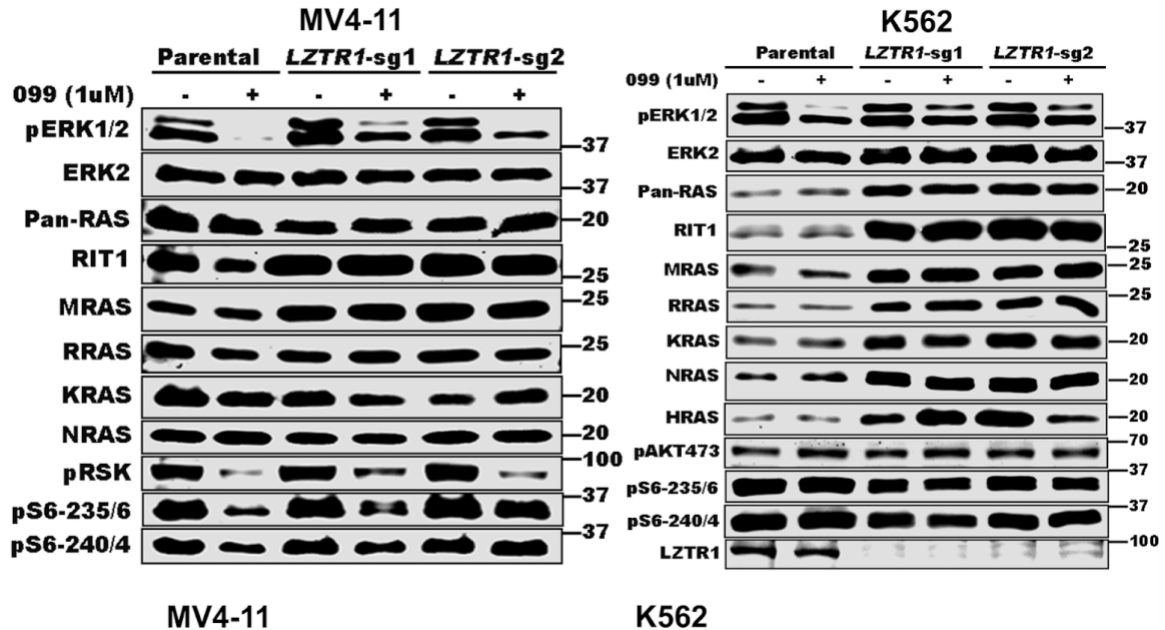


Figure 8. *LZTR1* KO has cell context-dependent effects on RIT1 and RAS family members. RIT1 and MRAS were upregulated in both MV4-11 and K562 *LZTR1* KO. However, only K562 *LZTR1* KO upregulated HRAS, KRAS, NRAS, Pan-RAS, and RRAS (W. Wei et al., 2023)

The results of Wei et al. (2023), shown in Figure 8, imply that RIT1 is a general substrate for *LZTR1*, as is MRAS, whereas other RAS family members are conditional substrates. The inhibition of ERK activation upon SHP2 inhibitor treatment was diminished in all *LZTR1* KO lines. However, the effect of *LZTR1* deficiency on the levels of RAS family members differed between K562 and MV4-11 cells. RIT1 KO reestablished SHP2 inhibitor sensitivity to both the *LZTR1* KO cell lines. (W. Wei et al., 2023). Wei et al. (2023) results indicate that, despite increasing multiple RAS family

members in *LZTR1* KO K562 cells, RIT1 is the primary driver of SHP2 inhibitor resistance.

Generation of *LZTR1*-TurboID fusion construct

To investigate the differential regulation of RAS proteins upon *LZTR1* KO. KO cell lines expressing Cas9 and the *LZTR1* sgRNA were mutated using plasmids obtained by Gibson Assembly. An sg-resistant *LZTR1* plasmid and TurboID plasmid were used as PCR templates for generating the inserts. The overlapping sequences on each inserts facilitated the fusion to the vector. Lentiviruses were generated using HEK 293T cells to infect MV-411 and K562 *LZTR1* KO cell lines. Dox inducible plasmids were used to control the expression of the protein of interest, reducing the background The expression of targeted proteins was demonstrated with Dox treatment in these cell lines (Figures 9 & 10).

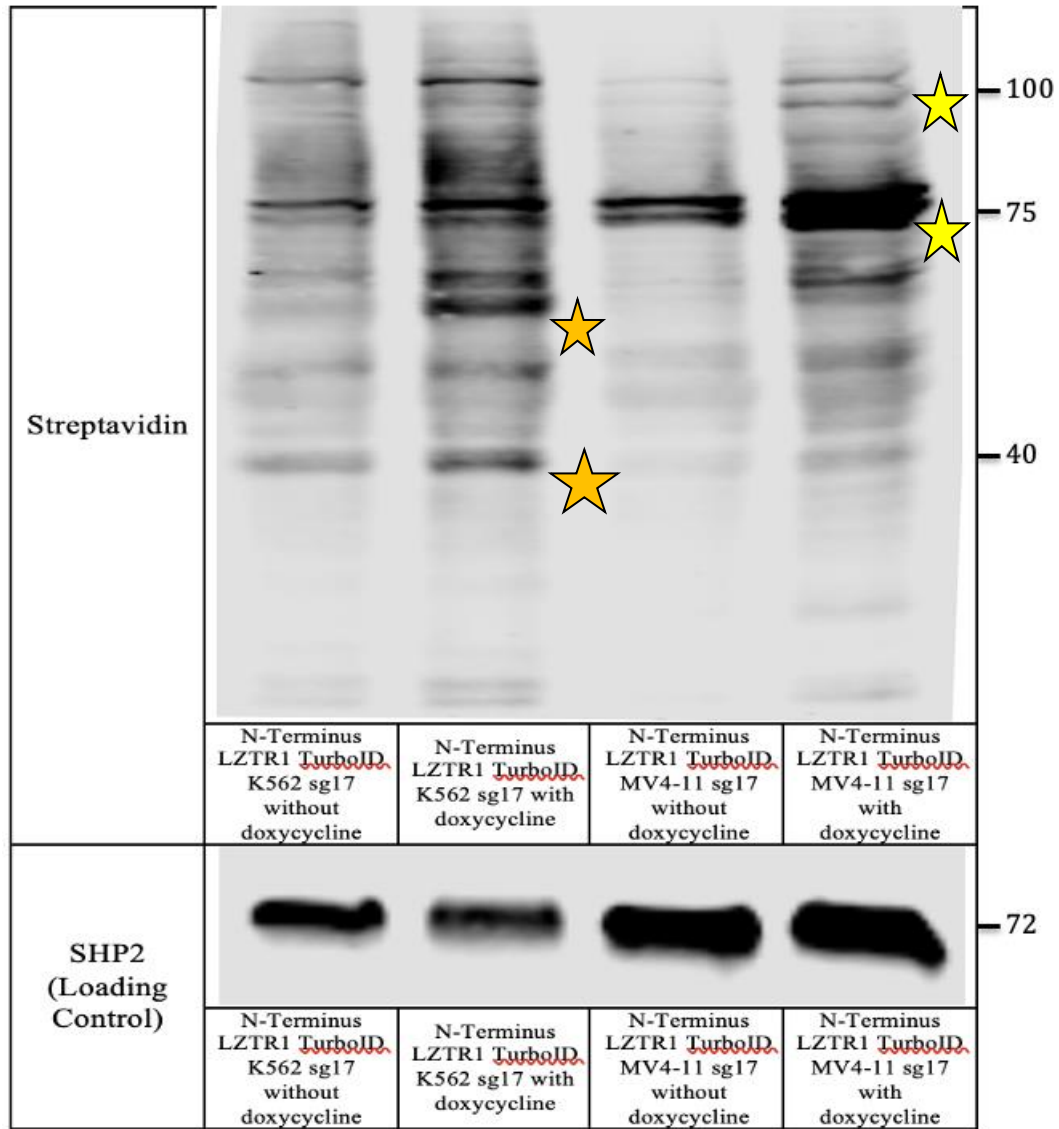


Figure 9. The addition of biotin increases labeling in N-terminal TurboID-expressing cells. Whole-cell lysates of K562 and MV4-11 cells expressing TurboID-tagged *LZTR1* proteins were analyzed via western blot in the presence of 50 μ M biotin supplementation for 15 minutes or in the absence of biotin supplementation. Streptavidin-HRP was used to probe for biotinylation. SHP2 was used as the loading control.

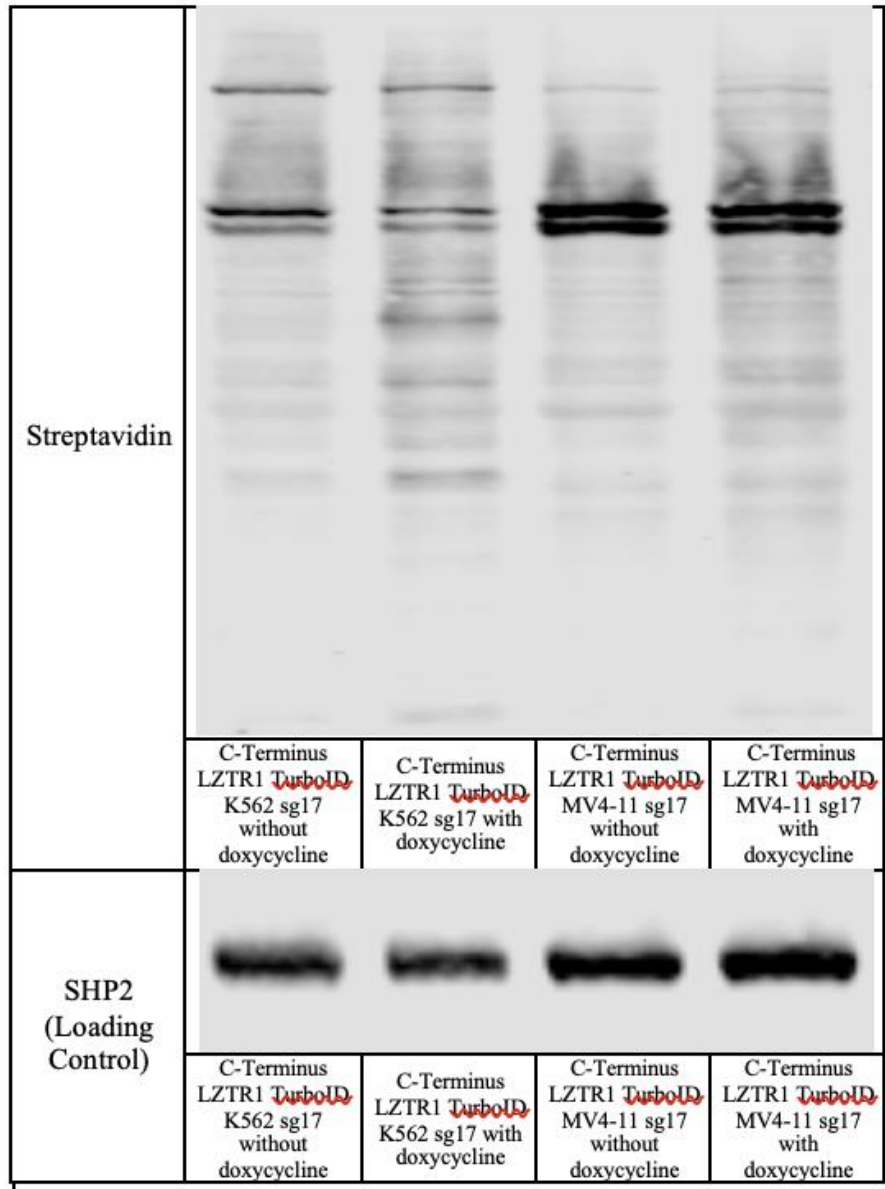


Figure 10. The addition of biotin had no significant effect on labeling in C-terminal TurboID-expressing cells. Whole-cell lysates of K562 and MV4-11 cells expressing TurboID-tagged *LZTR1* proteins were analyzed via western blot in the presence of 50 μ M biotin supplementation for 15 minutes or in the absence of biotin supplementation. Streptavidin-HRP was used to probe for biotinylation. SHP2 was used as the loading control.

When cells are tagged with TurboID, the biotin ligase fused to the protein of interest will biotinylate any nearby proteins. These biotinylated proteins can then be purified and identified by mass spectrometry. The increase of biotin labeling seen in TurboID-tagged cells results from the activity of the biotin ligase enzyme fused to the protein of interest, as shown in Figure 8. This enzyme catalyzes the covalent attachment of biotin to nearby proteins, increasing the amount of biotinylated proteins in the cell. The extent of biotinylation will depend on the expression level and localization of the TurboID-tagged protein, as well as the duration of the biotin labeling. Overall, the increase of biotin labeling seen in TurboID-tagged cells results from the biotin ligase activity of the TurboID fusion protein, which allows for the identification of protein interactors through mass spectrometry analysis.

The expression of LZTR1 was verified by plating the cells in biotin-free media and dox for three days. WT, KO, and TurboID cell lysates were collected and analyzed by western blot for LZTR1 expression. Unfortunately, the turboID labeled protein was not detected; only a weak signal from endogenous protein was observed. Due to a weak signal from endogenous protein, the next step was to investigate if TurboID fusions are functional by labeling them with biotin. The conditions tested were no dox and +dox+biotin. The N-terminal TurboID gave a much better signal upon biotinylation than the C-Terminal TurboID. There was little to no labeling in the C-Terminal Turbo ID.

In the C-Terminal TurboID, K562 had an extra band around 60 kDa and above 75, marked by the orange stars. Whereas the yellow stars mark MV4-11 additional bands

under 75 and 100 kDa. Although a mass spectrophotometer is needed to analyze these results further, it is very promising that patterns are different.

DISCUSSION

Unfortunately, due to time limitations, the TurboID-tagged cells have not yet been analyzed by mass spectrometry to identify potential *LZTR1* interactors. The findings align with prior research, highlighting *LZTR1*'s role in the RAS/MEK/ERK pathway and offering novel insights into its mode of action. As an adaptor for CUL3 E3 ligase complexes, *LZTR1* facilitates the degradation of target proteins. However, the target of the *LZTR1*/CUL3 complex has been debated. While initial research suggested RAS family members as targets, later studies proposed RIT1 as the primary substrate (Castel et al., 2019).

LZTR1 knockout (KO) consistently increased the expression of RIT1 and MRAS in both K562 and MV4-11 cells. Intriguingly, various RAS proteins were upregulated in other cell lines, with K562 cells exhibiting stabilization of KRAS, HRAS, NRAS, and RRAS. One potential explanation for these observations is that additional components within the *LZTR1*/CUL3 complexes are yet to be discovered. However, RIT1 deletion in *LZTR1*-KO K562 cells reestablishes SHP2 inhibitor sensitivity, suggesting that although *LZTR1* deficiency can influence other RAS family proteins in specific cells, RIT1 stabilization is essential for SHP2 inhibitor resistance.

Possible explanations for these findings are that an inhibitor of RAS ubiquitination in MV4-11 cells or a lack of positive molecule for RAS ubiquitination in MV4-11 cells and a presence of that molecule in K562 cells. Although this project mainly focused on identifying the binding partners of *LZTR1*, an alternative hypothesis would be the two cells expressed different isoforms of *LZTR1*.

The difference in labeling between N- and C-TurboID-tagged LZTR1 are most likely attributed to LZTR1 being unstable when tagged at the C-terminus. This finding might have resulted from using a 10 amino acid linker GGGSG x 2 between LZTR1 and TurboID, and this might not be long enough for the normal function of LZTR1. Glycine is also very prone to aggregation, so changing the linker sequence could improve expression. In the future, tests could be done to potentially reveal proteins that might be of interest in the proteomics screen.

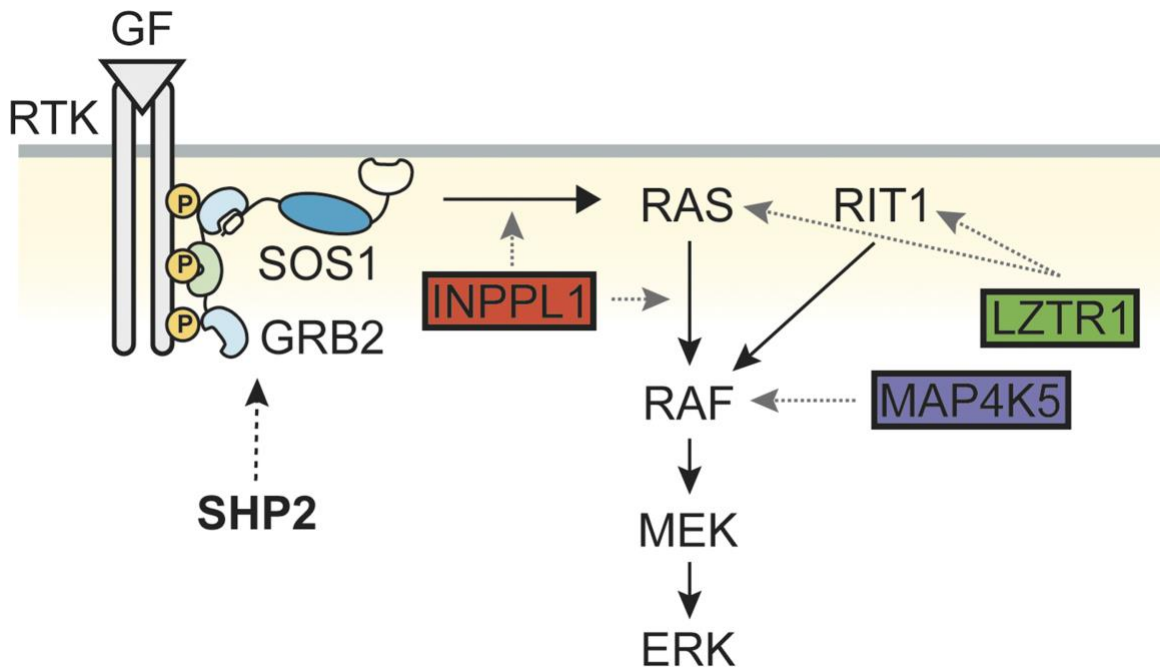


Figure 11. Model showing sites of action of *LZTR1*. *LZTR1* plays an effector role in RAS and RIT1 degradation. (W. Wei et al., 2023)

Additional *in vivo* and *in vitro* research is required to elucidate the hypothesized tissue-specific functions of different *LZTR1* isoforms, their cellular localization, and their interacting proteins to reveal the mechanisms contributing to schwannomas and other

tumor pathogenesis (Piotrowski et al., 2014). The data demonstrate that *LZTR1* has a negative regulatory role in controlling RAS function and MAPK signaling in various genetic diseases, such as Noonan syndrome (NS). Early detection may be more critical than treatment. Therefore, screening for *LZTR1* mutations and using RAS inhibitors could potentially prevent NS occurrence after birth. Similarly, for patients with *LZTR1* mutations in glioblastoma multiforme (GBM) and other cancers, RAS pathway inhibitors may be an effective treatment option. Thus, a comprehensive understanding of the different RAS activation mechanisms may benefit patients carrying *LZTR1* mutations and offer new therapeutic approaches.

The knowledge of *LZTR1* substrates remains incomplete. Protein interactions rely on their specific structures, and proteins that interact with the same partner often share similar domains. Identifying regions on known substrates that bind to *LZTR1* can accelerate research and help determine interacting domains in *LZTR1*-mediated substrates. Currently, *LZTR1* substrates are limited to the RAS superfamily, warranting further investigation into additional potential substrates.

Although *LZTR1* has traditionally been considered a ubiquitin-ligase enzyme rather than a phosphokinase, it regulates RAF1 phosphorylation without affecting its ubiquitination (Zhang et al., 2021b). *LZTR1* may mediate RAF1 phosphorylation by inducing PPP1CB ubiquitination in complexes, or it could phosphorylate substrates directly (Zhang et al., 2021a). However, this has not been confirmed. Examining the molecular basis for determining whether *LZTR1* can directly phosphorylate substrates is a valuable future research direction.

Mammalian genomes contain several genes encoding cullin proteins that form distinctive CRL subfamilies. Unlike other CRLs, CLR3 complexes have the unique feature of combining adaptor and receptor functions within a single protein, necessitating complex dimerization for catalytic activity. Typically, proteins that act as substrate receptors for CRL3 complexes possess a BTB/POZ region responsible for CUL3 binding and an additional domain for substrate recruitment. The process of substrate ubiquitination is achieved through the BTB domain, which facilitates the dimerization of two CRL3 complexes while concurrently engaging the substrate binding domains of both complexes with the substrate.

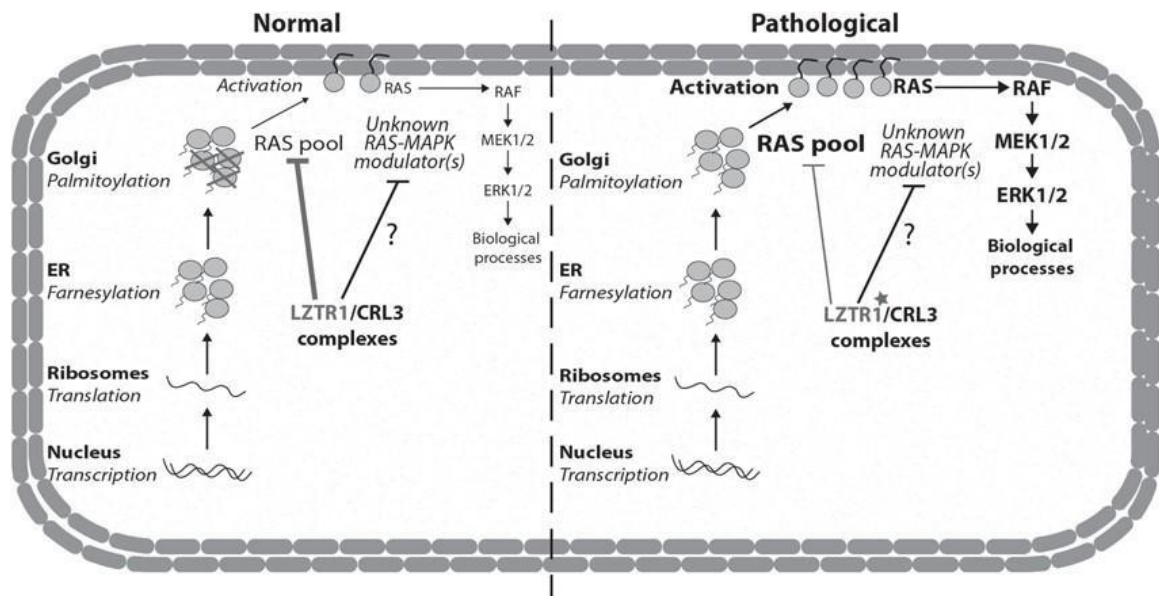


Figure 12. A proposed schematic showing *LZTR1* functioning in a CRL3 complex that down-regulates RAS-MAPK signaling. *LZTR1* is a substrate receptor for a CUL3 RING ligase (CLR3) complex regulating RAS levels. (Motta et al., 2019)

Moreover, *LZTR1* acts as a negative regulator inhibiting RAS function and MAPK signaling; mutations in this protein could disrupt RAS ubiquitination, reducing RAS superfamily protein turnover (Zhang et al., 2021). However, there is still conflicting evidence regarding *LZTR1*'s ability to bind to various members of the RAS and RRAS subfamilies, particularly the RIT1 and MRAS GTPases, as well as whether ubiquitination of these substrates results in their degradation.

LZTR1 might become an essential focus of biomedical research. Given its involvement in various human disorders, *LZTR1* is an attractive target for therapeutic interventions. Strategies could include gene therapy to replace or correct mutated *LZTR1* genes, small molecule inhibitors targeting critical components of the pathways in which *LZTR1* is involved, and immunotherapy approaches to boost the immune system's ability to target cells with dysfunctional *LZTR1*. However, developing these therapies will require a deeper understanding of the molecular mechanisms underlying *LZTR1* function and its role in disease. Additional research is necessary to understand better the biological function of *LZTR1* and its role in the incidence of diseases and the development of therapies, such as *LZTR1* promoters for patients with loss-of-function *LZTR1* mutations.

Several challenges must be addressed to fully understand the diverse roles of *LZTR1* in humans. These include the need for more comprehensive studies to uncover the molecular mechanisms of *LZTR1* function, the development of accurate animal models, and the identification of reliable biomarkers for early detection and disease monitoring. Additionally, understanding the regulation of *LZTR1* expression, localization, and post-translational modifications could provide valuable information on how its function is

controlled in different cellular contexts. Overall, the challenges to *LZTR1* research highlight the importance of continued study and exploration of this gene's role in cellular processes and the need for innovative approaches to diagnosing and treating associated disorders.

BIBLIOGRAPHY

- Abe, T., Umeki, I., Kanno, S.-I., Inoue, S.-I., Niihori, T., & Aoki, Y. (2020). LZTR1 facilitates polyubiquitination and degradation of RAS-GTPases. *Cell Death and Differentiation*, 27(3), 1023–1035. <https://doi.org/10.1038/s41418-019-0395-5>
- Aoki, Y., Niihori, T., Inoue, S., & Matsubara, Y. (2016). Recent advances in RASopathies. *Journal of Human Genetics*, 61(1), 33–39. <https://doi.org/10.1038/jhg.2015.114>
- Avilan, L. (2023). Assembling Multiple Fragments: The Gibson Assembly. *Methods in Molecular Biology*, 2633, 45–53. https://doi.org/10.1007/978-1-0716-3004-4_4
- Barbosa, C., Nogueira, S., Gadanho, M., & Chaves, S. (2016). Chapter 7 - DNA extraction: Finding the most suitable method. In N. Cook, M. D'Agostino, & K. C. Thompson (Eds.), *Molecular Microbial Diagnostic Methods* (pp. 135–154). Academic Press. <https://doi.org/10.1016/B978-0-12-416999-9.00007-1>
- Barford, D., & Neel, B. G. (1998). Revealing mechanisms for SH2 domain mediated regulation of the protein tyrosine phosphatase SHP-2. *Structure*, 6(3), 249–254. [https://doi.org/10.1016/S0969-2126\(98\)00027-6](https://doi.org/10.1016/S0969-2126(98)00027-6)
- Bigenzahn, J. W., Collu, G. M., Kartnig, F., Pieraks, M., Vladimer, G. I., Heinz, L. X., Sedlyarov, V., Schischlik, F., Fauster, A., Rebsamen, M., Parapatics, K., Blomen, V. A., Müller, A. C., Winter, G. E., Kralovics, R., Brummelkamp, T. R., Mlodzik, M., & Superti-Furga, G. (2018). LZTR1 is a regulator of RAS ubiquitination and signaling. *Science*, 362(6419), 1171–1177. <https://doi.org/10.1126/science.aap8210>

- Branon, T. C., Bosch, J. A., Sanchez, A. D., Udeshi, N. D., Svinkina, T., Carr, S. A., Feldman, J. L., Perrimon, N., & Ting, A. Y. (2017). *Directed evolution of TurboID for efficient proximity labeling in living cells and organisms* [Preprint]. Bioengineering. <https://doi.org/10.1101/196980>
- Branon, T. C., Bosch, J. A., Sanchez, A. D., Udeshi, N. D., Svinkina, T., Carr, S. A., Feldman, J. L., Perrimon, N., & Ting, A. Y. (2018). Efficient proximity labeling in living cells and organisms with TurboID. *Nature Biotechnology*, 36(9), Article 9. <https://doi.org/10.1038/nbt.4201>
- Castel, P. (2022). Defective protein degradation in genetic disorders. *Biochimica et Biophysica Acta (BBA) - Molecular Basis of Disease*, 1868(5), 166366. <https://doi.org/10.1016/j.bbadis.2022.166366>
- Castel, P., Cheng, A., Cuevas-Navarro, A., Everman, D. B., Papageorge, A. G., Simanshu, D. K., Tankka, A., Galeas, J., Urisman, A., & McCormick, F. (2019). RIT1 oncoproteins escape LZTR1-mediated proteolysis. *Science*, 363(6432), 1226–1230. <https://doi.org/10.1126/science.aav1444>
- Chan, G., Kalaitzidis, D., & Neel, B. G. (2008). The tyrosine phosphatase Shp2 (PTPN11) in cancer. *Cancer and Metastasis Reviews*, 27(2), 179–192. <https://doi.org/10.1007/s10555-008-9126-y>
- Chen, R.-H. (2020). Cullin 3 and Its Role in Tumorigenesis. In Y. Sun, W. Wei, & J. Jin (Eds.), *Cullin-RING Ligases and Protein Neddylation: Biology and Therapeutics* (pp. 187–210). Springer. https://doi.org/10.1007/978-981-15-1025-0_12

- Cho, K. F., Branon, T. C., Rajeev, S., Svinkina, T., Udeshi, N. D., Thoudam, T., Kwak, C., Rhee, H.-W., Lee, I.-K., Carr, S. A., & Ting, A. Y. (2020). Split-TurboID enables contact-dependent proximity labeling in cells. *Proceedings of the National Academy of Sciences of the United States of America*, *117*(22), 12143–12154. <https://doi.org/10.1073/pnas.1919528117>
- Cho, K. F., Branon, T. C., Udeshi, N. D., Myers, S. A., Carr, S. A., & Ting, A. Y. (2020). Proximity labeling in mammalian cells with TurboID and split-TurboID. *Nature Protocols*, *15*(12), Article 12. <https://doi.org/10.1038/s41596-020-0399-0>
- Cuevas-Navarro, A., Rodriguez-Muñoz, L., Grego-Bessa, J., Cheng, A., Rauen, K. A., Urisman, A., McCormick, F., Jimenez, G., & Castel, P. (2022). Cross-species analysis of LZTR1 loss-of-function mutants demonstrates dependency to RIT1 orthologs. *eLife*, *11*, e76495. <https://doi.org/10.7554/eLife.76495>
- Cuevas-Navarro, A., Van, R., Cheng, A., Urisman, A., Castel, P., & McCormick, F. (2021). The RAS GTPase RIT1 compromises mitotic fidelity through spindle assembly checkpoint suppression. *Current Biology: CB*, *31*(17), 3915-3924.e9. <https://doi.org/10.1016/j.cub.2021.06.030>
- Damnernsawad, A., Bottomly, D., Kurtz, S. E., Eide, C. A., McWeeney, S. K., Tyner, J. W., & Nechiporuk, T. (2022). Genome-wide CRISPR screen identifies regulators of MAPK and MTOR pathways mediating sorafenib resistance in acute myeloid leukemia. *Haematologica*, *107*(1), 77–85. <https://doi.org/10.3324/haematol.2020.257964>

Farncombe, K. M., Thain, E., Barnett-Tapia, C., Sadeghian, H., & Kim, R. H. (2022).

LZTR1 molecular genetic overlap with clinical implications for Noonan syndrome and schwannomatosis. *BMC Medical Genomics*, *15*(1), 160.

<https://doi.org/10.1186/s12920-022-01304-x>

Garibyan, L., & Avashia, N. (2013). Research Techniques Made Simple: Polymerase

Chain Reaction (PCR). *The Journal of Investigative Dermatology*, *133*(3), e6.

<https://doi.org/10.1038/jid.2013.1>

Gibson, D. G., Young, L., Chuang, R.-Y., Venter, J. C., Hutchison, C. A., & Smith, H. O.

(2009). Enzymatic assembly of DNA molecules up to several hundred kilobases.

Nature Methods, *6*(5), Article 5. <https://doi.org/10.1038/nmeth.1318>

Güemes, M., Martín-Rivada, Á., Ortiz-Cabrera, N. V., Martos-Moreno, G. Á., Pozo-

Román, J., & Argente, J. (2019). LZTR1: Genotype Expansion in Noonan

Syndrome. *Hormone Research in Paediatrics*, *92*(4), 269–275.

<https://doi.org/10.1159/000502741>

Guo, Y.-J., Pan, W.-W., Liu, S.-B., Shen, Z.-F., Xu, Y., & Hu, L.-L. (2020). ERK/MAPK

signalling pathway and tumorigenesis (Review). *Experimental and Therapeutic*

Medicine, *19*(3), 1997–2007. <https://doi.org/10.3892/etm.2020.8454>

Isothermal Reaction (Gibson Assembly) Master Mix. (2017). *Cold Spring Harbor*

Protocols, *2017*(3), pdb.rec090019. <https://doi.org/10.1101/pdb.rec090019>

Ko, A., Hasanain, M., Oh, Y. T., D'Angelo, F., Sommer, D., Frangaj, B., Tran, S., Bielle,

F., Pollo, B., Pattera, R., Mokhtari, K., Soni, R. K., Peyre, M., Eoli, M., Papi, L.,

Kalamarides, M., Sanson, M., Iavarone, A., & Lasorella, A. (2023). LZTR1

- Mutation Mediates Oncogenesis through Stabilization of EGFR and AXL. *Cancer Discovery*, 13(3), 702–723. <https://doi.org/10.1158/2159-8290.CD-22-0376>
- Mohi, M. G., & Neel, B. G. (2007). The role of Shp2 (PTPN11) in cancer. *Current Opinion in Genetics & Development*, 17(1), 23–30. <https://doi.org/10.1016/j.gde.2006.12.011>
- Motta, M., Fidan, M., Bellacchio, E., Pantaleoni, F., Schneider-Heieck, K., Coppola, S., Borck, G., Salviati, L., Zenker, M., Cirstea, I. C., & Tartaglia, M. (2019). Dominant Noonan syndrome-causing LZTR1 mutations specifically affect the Kelch domain substrate-recognition surface and enhance RAS-MAPK signaling. *Human Molecular Genetics*, 28(6), 1007–1022. <https://doi.org/10.1093/hmg/ddy412>
- Nacak, T. G., Leptien, K., Fellner, D., Augustin, H. G., & Kroll, J. (2006). The BTB-kelch protein LZTR-1 is a novel Golgi protein that is degraded upon induction of apoptosis. *The Journal of Biological Chemistry*, 281(8), 5065–5071. <https://doi.org/10.1074/jbc.M509073200>
- Neel, B. G., Gu, H., & Pao, L. (2003). The 'Shp'ing news: SH2 domain-containing tyrosine phosphatases in cell signaling. *Trends in Biochemical Sciences*, 28(6), 284–293. [https://doi.org/10.1016/S0968-0004\(03\)00091-4](https://doi.org/10.1016/S0968-0004(03)00091-4)
- Paladino, A., D'Angelo, F., Noviello, T. M. R., Iavarone, A., & Ceccarelli, M. (2021). Structural Model for Recruitment of RIT1 to the LZTR1 E3 Ligase: Evidences from an Integrated Computational Approach. *Journal of Chemical Information and Modeling*, 61(4), 1875–1888. <https://doi.org/10.1021/acs.jcim.1c00296>

Park, J., Cho, J., & Song, E. J. (2020). Ubiquitin–proteasome system (UPS) as a target for anticancer treatment. *Archives of Pharmacal Research*, 43(11), 1144–1161.

<https://doi.org/10.1007/s12272-020-01281-8>

Piotrowski, A., Xie, J., Liu, Y. F., Poplawski, A. B., Gomes, A. R., Madanecki, P., Fu, C., Crowley, M. R., Crossman, D. K., Armstrong, L., Babovic-Vuksanovic, D., Bergner, A., Blakeley, J. O., Blumenthal, A. L., Daniels, M. S., Feit, H., Gardner, K., Hurst, S., Kobelka, C., ... Messiaen, L. M. (2014). Germline loss-of-function mutations in LZTR1 predispose to an inherited disorder of multiple schwannomas. *Nature Genetics*, 46(2), 182–187. <https://doi.org/10.1038/ng.2855>

PubChem. (n.d.). *LZTR1—Leucine zipper like transcription regulator 1 (human)*.

Retrieved March 26, 2023, from

<https://pubchem.ncbi.nlm.nih.gov/gene/LZTR1/human>

Qin, W., Cho, K. F., Cavanagh, P. E., & Ting, A. Y. (2021). Deciphering molecular interactions by proximity labeling. *Nature Methods*, 18(2), Article 2.

<https://doi.org/10.1038/s41592-020-01010-5>

Shioya, R., Yamada, K., Kido, K., Takahashi, H., Nozawa, A., Kosako, H., & Sawasaki, T. (2022). A simple method for labeling proteins and antibodies with biotin using the proximity biotinylation enzyme TurboID. *Biochemical and Biophysical Research Communications*, 592, 54–59. <https://doi.org/10.1016/j.bbrc.2021.12.109>

Tartaglia, M., Aoki, Y., & Gelb, B. D. (2022). The molecular genetics of RASopathies: An update on novel disease genes and new disorders. *American Journal of Medical*

Genetics. Part C, Seminars in Medical Genetics, 190(4), 425–439.

<https://doi.org/10.1002/ajmg.c.32012>

Wei, W., Geer, M. J., Guo, X., Dolgalev, I., Sanjana, N. E., & Neel, B. G. (2023).

Genome-wide CRISPR/Cas9 screens reveal shared and cell-specific mechanisms of resistance to SHP2 inhibition. *The Journal of Experimental Medicine*, 220(5), e20221563. <https://doi.org/10.1084/jem.20221563>

Wei, X.-F., Li, S., & Hu, J.-L. (2023). A TurboID-based proximity labelling approach for identifying the DNA-binding proteins. *STAR Protocols*, 4(1), 102139.

<https://doi.org/10.1016/j.xpro.2023.102139>

Young, L., Sung, J., Stacey, G., & Masters, J. R. (2010). Detection of Mycoplasma in cell cultures. *Nature Protocols*, 5(5), Article 5. <https://doi.org/10.1038/nprot.2010.43>

Yuan, J., Dong, X., Yap, J., & Hu, J. (2020). The MAPK and AMPK signalings: Interplay and implication in targeted cancer therapy. *Journal of Hematology & Oncology*, 13(1), 113. <https://doi.org/10.1186/s13045-020-00949-4>

Zhang, H., Cao, X., Wang, J., Li, Q., Zhao, Y., & Jin, X. (2021). LZTR1: A promising adaptor of the CUL3 family. *Oncology Letters*, 22(1), 564.

<https://doi.org/10.3892/ol.2021.12825>

Zhou, B., Ying, X., Chen, Y., & Cai, X. (2022). A Comprehensive Pan-Cancer Analysis of the Tumorigenic Effect of Leucine-Zipper-Like Transcription Regulator (LZTR1) in Human Cancer. *Oxidative Medicine and Cellular Longevity*, 2022, 2663748.

<https://doi.org/10.1155/2022/2663748>

CURRICULUM VITAE

